

Influence of ZnO Nanoparticle coatings on Corrosion Protection of API5 CT N80 and API 5L Grade B Steel in Albian water

Fatiha Chelgham

Laboratoire de Valorisation et Promotion des Ressources Sahariennes, Université Kasdi Merbah, Ouargla - 30000, Algerie

Adel Taabouche

Thin Films and Interfaces Laboratory, University of Frères Mentouri Constantine, Constantine, 25000 Algeria.

Brahim Gharbi

Faculté des hydrocarbures, énergies renouvelables, science de la terre et de l'univers, Université Kasdi Merbah, Ouargla-30000, Algerie.

Amira Ouakkaf

Faculté des sciences exactes, Université Mohamed Khider, Biskra,07000, Algerie.

Khadra Mokadem

Laboratoire de Valorisation et Promotion des Ressources Sahariennes, Université Kasdi Merbah, Ouargla - 30000, Algerie.

Mounira Chelgham

Développement des énergies nouvelles et renouvelables dans les zones arides et sahariennes, LENREZA, P.O. Box 511, Ouargla 30 000, Algeria

Souheyla Boudjema

Département de chimie, Laboratoire de catalyse et synthèse en chimie organique, Université de Tlemcen, Tlemcen, Algérie.

Fares Mohammed Laid Rekbi

Scientific and Technical Research Center in Physico-Chemical Analysis (CRAPC), Algeria.

Mohammed Amine Fellah

Faculté des hydrocarbures, énergies renouvelables, science de la terre et de l'univers, Université Kasdi Merbah, Ouargla-30000, Algerie.

Mohammed Elazhri Charef

Faculté des hydrocarbures, énergies renouvelables, science de la terre et de l'univers, Université Kasdi Merbah, Ouargla-30000, Algerie.

Abstract

In petroleum industry such as pipe line, Corrosion increases a risk of structural failure, by reducing the steel's ability to support weight, It raises the expense of replacement and expensive substitutes. This study looks at how thin-film zinc oxide coatings affect the shape and corrosion rate of two different steels, API 5CT N80 and API 5L GRADE B. Zinc acetate was used to create ZnO thin films using Spray Pyrolysis (SP), which were subsequently applied to heated and cleaned carbon steel substrates. While energy dispersive X-ray spectroscopy (EDX) revealed the presence of Zn and O in the coatings, scanning electron microscopy (SEM) analysis proved the presence of homogenous, uniform layers. Furthermore, Fourier transform infrared spectroscopy (FTIR) is used to confirm the development of ZnO nanocrystals on surfaces. The ZnO thin film's hardness test has shown that it is suitable and long-lasting as a protective surface layer. With efficiencies of 88.60% and 95.39%, respectively, the coated films improved the corrosion resistance of API 5CT N80 and API 5L Grade B steels.

Key Words: Spray Pyrolysis, Substrate, Thin film ZnO, corrosion, Carbon steel.

1. Introduction

One of the most popular materials in industry for transporting gas, oil, and water is carbon steel. Carbon steel pipeline corrosion is a severe issue that has led to multiple failures. (Heakal et al 2018; Liu et al.2016; Usher et al.2014 ; Chen et al. 2012). The integrity of metals such as carbon steel used in pipeline networks can be severely damaged by production water, causing serious corrosion problems (Benamor et al.2018). However, oil pipeline failures cause huge economic losses (Cheng et al. 2012 ; Alamilla et al. 2013) , and the industry spends the equivalent of millions of pounds per year to repair the damage (Tang et al. 2009; Zhang and Katz 2010) .

Without corrosion inhibitors, corrosion rates can reach very high levels (>100 mm/year) and rise rapidly as the temperature and acid concentration rise (Finšgar and Jackson 2014; Barmatov et al. 2012) .Production water's impact on the corrosion behavior of petroleum sector equipment and pipelines has drawn attention from all around the world (Jordan et al. 2001; Migahed et al.2015) .

According to Finšgar et al. (2014), API N80 (American Petroleum Institute) carbon steel is typically utilized as the primary building material for drill pipes and Pipes used for transportation in the petroleum sector (Yadav et al. 2016; Vishwanatham and Haldar 2008; Zhu et al.2011), according to Finšgar et al. (2014). Although corrosion is unavoidable, it can be managed (Heakal and Elkholy 2017) using a variety of techniques, including corrosion inhibitors (Verma et al. 2017), metal coatings (Nagarajan et al.2012), and cathodic protection (Peabody 2001) .In the petroleum sector, carbon steel known as API N80 (American Petroleum Institute) is typically utilized as the primary building material for drill pipes and transit pipelines (Yadav et al. 2016;Vishwanatham and Haldar 2008; Zhu et al. 2011). Although corrosion is unavoidable, it can be managed (Heakal and Elkholy 2017) using a variety of techniques, including corrosion inhibitors (Verma et al. 2017), metal coatings (Nagarajan et al. 2012), and cathodic protection (Peabody 2001) .

The structural and electrical properties of ZnO under various pressure settings were investigated by Benkrima et al. (2022). The point at which crystalline ZnO changes from the wurtzite phase to the rock salt phase at 13.38 GPa of pressure was also determined by the study.

Owoeye et al. (2025) show that investigates the effect of zinc oxide thin-film coatings on mild steel's shape and rate of corrosion. Energy dispersive X-ray spectroscopy (EDX) showed the existence of Zn and O in the coatings, while scanning electron microscopy (SEM) examination verified the development of uniform, defect-free layers using chemical spray pyrolysis. The mild steel's resistance to corrosion was improved by the coated coatings.

Thin film ZnO on carbon steels API 5 CT N80 and API 5 CL Grad B behavior in albian water (aquifer water) obtained from the Haoud-Berkaoui area, which is roughly 100 km west of Hassi-Messaoud (Algeria), is the main subject of this study.The electrochemical behavior was examined using potentiodynamic polarization.

2. Experimental

2.1 Materials

The study's mild steel substrates, API 5 CT N80 and API 5L Grade B, were from Haoud-Berkaoui in south Algeria. The Samples were machined and sliced into 1 cm².

The liquid precursors were made with distilled water and commercially available zinc acetate. The deposition method used was chemical spray pyrolysis.

The characteristics of the generated water, which has an average pH of 7.79, are provided in Table 1 to help comprehend the chemical makeup of the albian water utilized in the studies.

Table 1. The chemical composition of albian water.

Elements	Ca+2	Mg+2	Na+	K+	Cl-	SO ₄ ²⁻	HCO ₃ ⁻	NO ₃ ⁻	pH
Composition (mg/l)	175.56	92.82	284.28	33	526.85	561.14	150.14	11.85	7.79

2.2 Preparation of Thin film and Characterizations

One hundred and nine percent pure zinc acetate (Zn(CH₃COO)₂·2H₂O) was employed to create the liquid precursor for ZnO films. Using the method outlined in Refs. [23-26], The precursors were produced in distilled water at a concentration of 0.1 M.. Spray pyrolysis was used to apply precursors to a mild steel substrate that had been cleaned and heated beforehand.

The generated films were characterized using scanning electron microscopy (SEM) and energy dispersive X-ray spectroscopy (EDX) to ascertain their shape and elemental makeup.

Fourier Transform Infrared Spectroscopy (FTIR) was used to identify the presence of functional groups in the thin film within the 400–4000 cm⁻¹ range. ZnO/Fe Particle Morphology and Substratum Surface

A Vickers microhardness tester (System Zwick) was used to conduct hardness tests for mechanical characterisation of the ZnO-coated substrates. Five indentations were made for 15 seconds at a force of 1000g

2.3 Electrochemical analysis of coated substrates

A PC running VoltaMaster-4 software connected to a potentiostat/galvanostat Type PGZ 301 was used to conduct the electrochemical measurements. There was albian water in the test solutions. An electrode that had been mechanically polished was utilized for every measurement. Emery sheets of progressively finer grades (grades 200–2000) were used for polishing. At a scan rate of 30 mV/min, the polarization curves (Tafel plots) were conducted at an open circuit voltage range of -300 to -900 mV. Room temperature was used for the electrochemical measurements.

3. Results and discussion

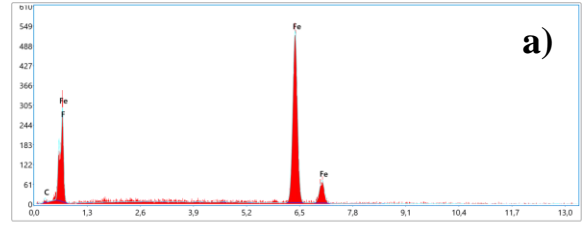
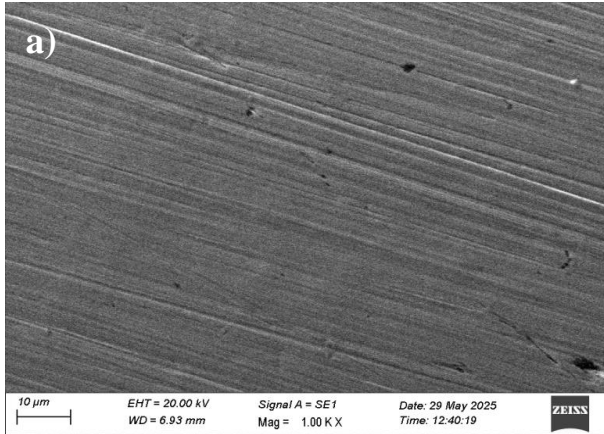
3.1 Microstructure of the carbon steel sample

The microscopic SEM images of the samples are shown in Fig. 1 for API 5 CL Grade B and Fig.. 2 for API 5 CT N80 with and without ZnO thin layer. The microscopic SEM images of Fig. 1.a and Fig. 2.a. Nothing is visible on the surface. While the microscopic images of Fig. 1.b and Fig. 2.b. show numerous grains in the structure, that there is substitutional diffusion of zinc oxide thin layers into the carbon steel substrates, that these grains were coated with layers as evidence of surface modification. It was observed that the surface morphology of mild steel was improved by the ZnO coating. It was observed that the coated layers adhered effectively to the substrates and a good growth of the substrate surface was visible (Owoeye et al. 2023).

Fig.1 and Fig. 2 also show the EDX spectra of the samples. The component peaks of some selected areas the EDX spectra, which show the SEM micrographs. The presence of Fe and C in the samples without ZnO because that the major components of carbon steels.

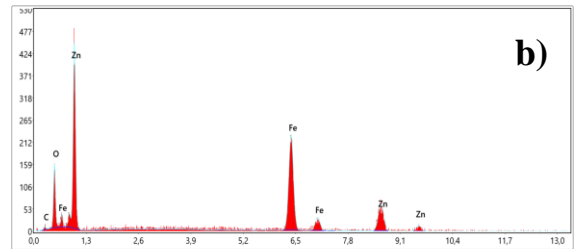
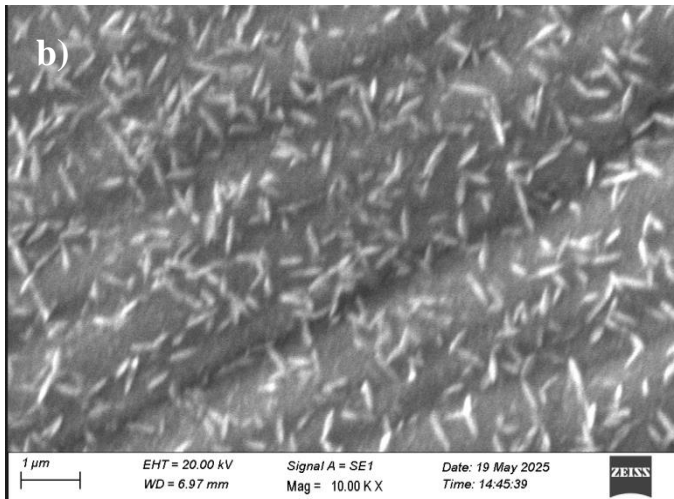
However, the spectra of Fig. 1.b and Fig. 2.b verify the existence of O and Zn deposits in the deposited layers. , as shown by the reduction of Fe composition. This means that the thin ZnO layers suppressed the signal of Fe content in carbon steel, which primarily affects the corrosion resistance of the material.

A protective oxide layer is created when coated ZnO reacts with O on the surface, altering its structure and lowering the quantity of free Zn and O present.. With reduced interaction with ambient oxygen, coated films provide more stable and protective layers (Owoeye et al. 2025).



Element	Wt (%)
C	2.39
Fe	95.02

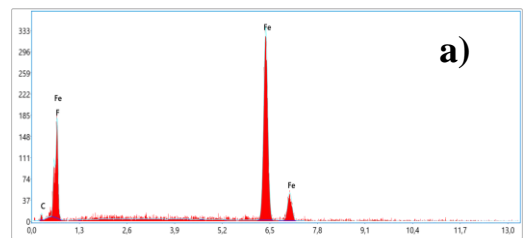
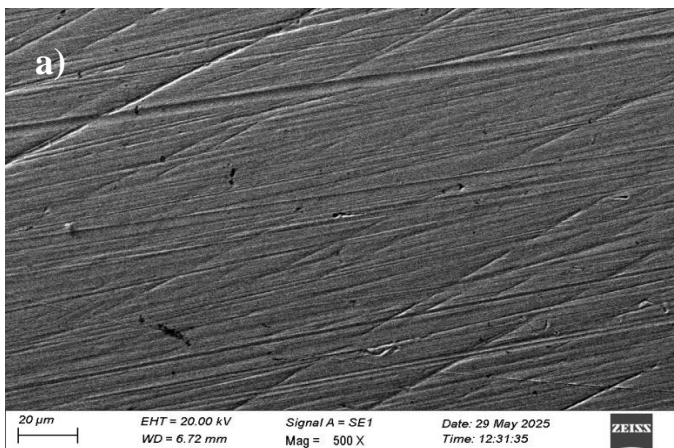
EDS analysis



Element	Wt (%)
C	2.39
O	11.57
Fe	51.98
Zn	34.06

EDS analysis

Fig. 1. Surface micrographs and EDS Spectra of API 5CL Grade B , a) without ZnO and b) with ZnO.



Element	Wt (%)
C	10.33
Fe	78.77

EDS analysis

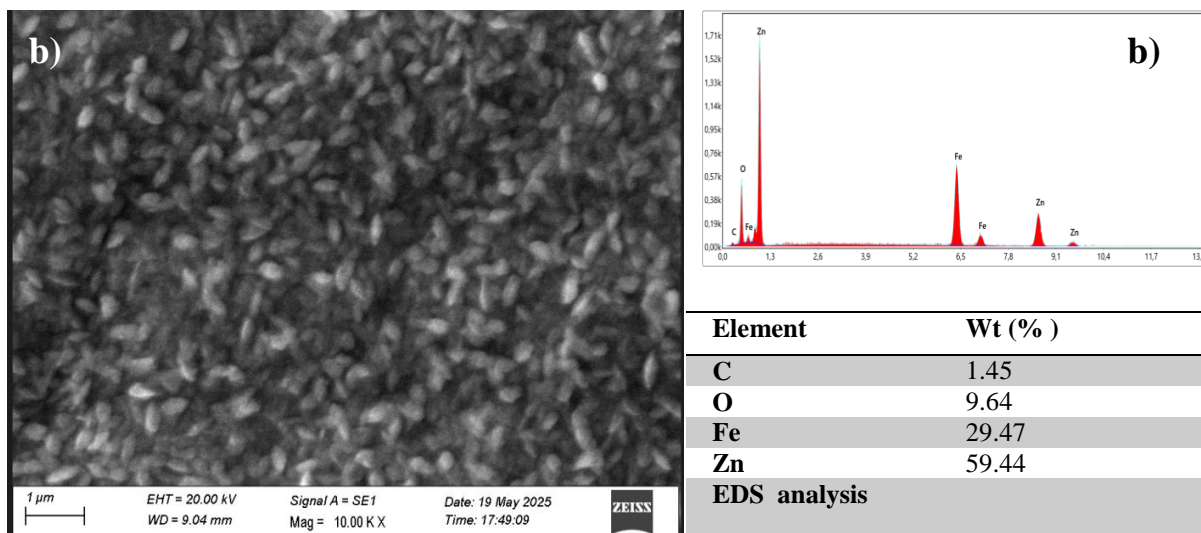


Fig. 2. Surface micrographs and EDS Spectra of API 5CT N80 , a) without ZnO and b) with ZnO

3.2 FTIR studies

FTIR analysis is an analysis that uses the absorption of infrared radiation. You can describe the material's general chemical properties since each of its functional groups absorbs a different spectrum. The results of FTIR tests are shown as graphs with several absorption peaks that indicate the compounds present.

The FTIR spectra of API Grade B steel, both untreated (a) and ZnO-coated (b), are displayed in Fig. 3. These spectra highlight significant variations in surface chemistry. A pristine metallic surface with little oxidation is indicated by the uncoated sample's comparatively flat spectrum with mild absorption bands. Fe–O stretching vibrations are responsible for a large signal below 700 cm^{-1} , indicating the presence of native iron oxide (Xu et al. 2008). On the other hand, the ZnO-coated sample shows a noticeable absorption band in the $500\text{--}600\text{ cm}^{-1}$ range, which is indicative of Zn–O bond vibrations and validates that ZnO was successfully deposited (Thirugnanam 2013; Rao and Rao 2015; Quadri et al. 2017). At higher wavenumbers ($3000\text{--}3500\text{ cm}^{-1}$), the coated surface also exhibits less fluctuation in transmittance, indicating less surface –OH adsorption and enhanced moisture resistance. The ZnO coating alters the surface, improving corrosion resistance and creating a more stable, passivated layer, as shown by these spectrum differences.

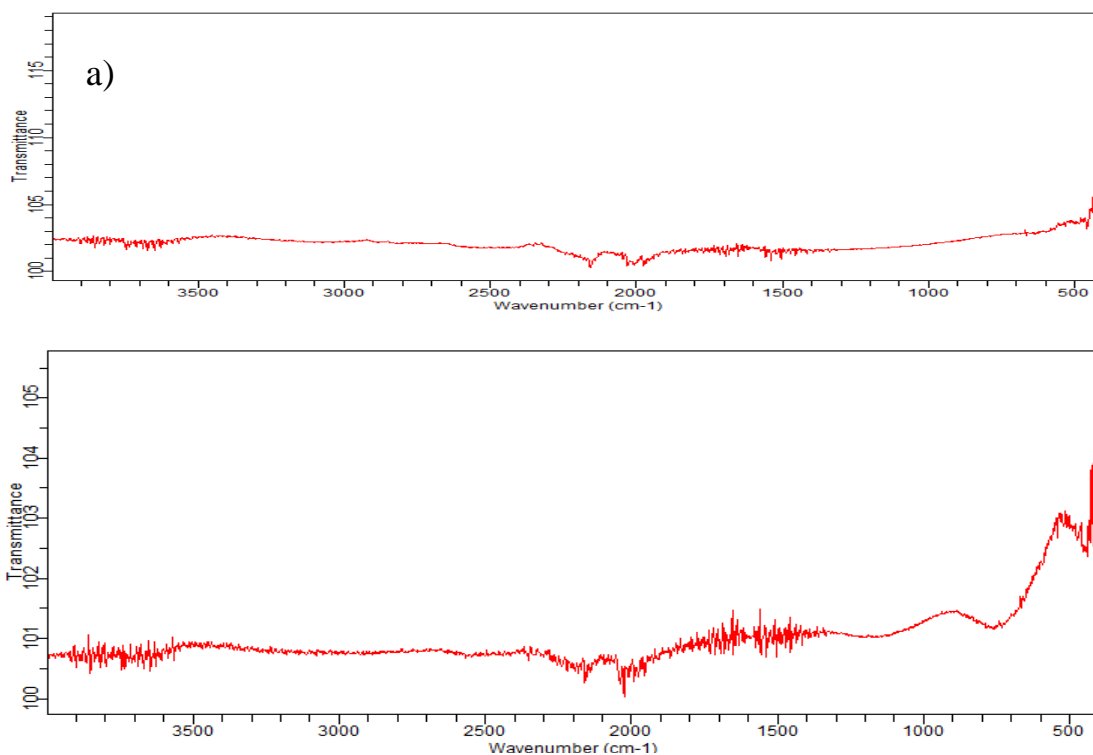


Fig. 3 . FTIR spectra of API Grade B steel (a) uncoated surface (b) surface coated with ZnO thin film.

Comparative FTIR Analysis of ZnO-Coated and Uncoated API 5CL N80 Steel

Significant variations in surface chemistry are revealed by the FTIR spectra of API 5CT N80 steel, both untreated (a) and coated with ZnO (b), as shown in Fig. 4. Broad absorption characteristics are seen in the uncoated sample (a), including a shoulder at 3400 cm^{-1} that can be caused by moisture or surface -OH groups (Raja et al.2014 ; Tu et al.2025), and faint bands around $2100\text{--}2000\text{ cm}^{-1}$ that might be signs of adsorbed CO_2 or surface carbonates (Kö ck et al. 2013).

The area between 1500 and 500 cm^{-1} : Crucial in metals:

Natural oxidation of the steel surface is indicated by a broad signal compatible with Fe-O vibrations in the range below 700 cm^{-1} (Pujari et al.2025) . The ZnO-coated sample (b), on the other hand, shows more distinct peaks, especially a distinct band that corresponds to Zn-O stretching vibrations and is located between 500 and 600 cm^{-1} . The coating suggests a more stable and protected surface by lessening the intensity of other surface details. This comparison demonstrates how the ZnO layer changes the surface composition of steel, improving its resistance to corrosion and chemical passivation in harsh situations.

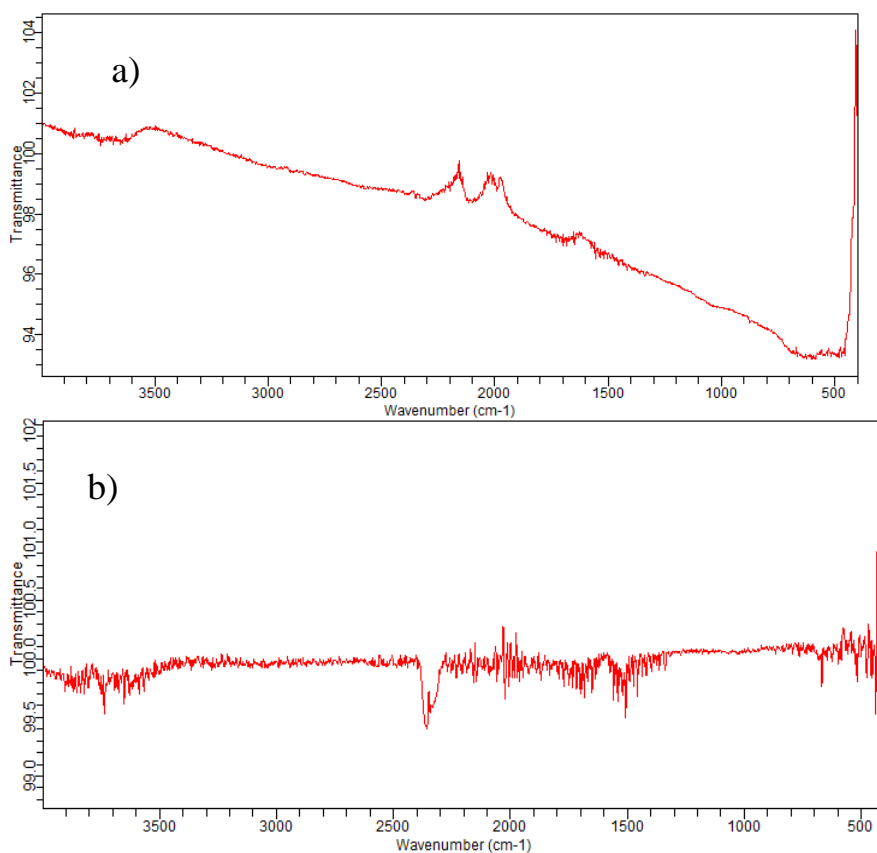


Fig. 4 . FTIR spectra of API 5CL N80 steel (a) uncoated surface (b) surface coated with ZnO thin film

3.3 The hardness test

Since hardness shows resistance to localized plastic deformation, it is an essential property to evaluate. The microhardness of API 5CT N80 and API 5L Grade B steels was measured before and after the deposition of a ZnO thin film using the Vickers hardness test. As shown in Table 2, the untreated API 5CT N80 exhibited a hardness of 176.7 HV , which significantly increased to 278.3 HV after ZnO coating . Similarly, API 5L Grade B showed a modest increase in hardness from 176.78 HV to 184.48 HV following ZnO deposition. This improvement in surface hardness confirms the mechanical reinforcement provided by the ZnO thin film, which enhances the wear resistance and durability of the steel substrates (Xu et al. 2008; Chikodi et al. 2021) .

Table 2. Microhardness values before and after coating thin film ZnO.

Steel	Hardness (HV)
API 5T N80 untreated	176.7
API 5T N80 with ZnO	278.3
API 5L Grade B untreated	176.78
API 5L Grade B with ZnO	184.48

3.4 Potentiodynamic Polarization measurements

The FTIR spectrum Fig.5 displays the Tafel curves for ZnO-coated steel and pure steel. A mixed-type coating is indicated by the anodic and cathodic curves being shifted to lower current densities with the thin film ZnO (John et al. 2015).

Additionally, the curves were moved to higher potential regions by the coated substrates, suggesting that corrosion was slowing down (Castro et al. 2025). The parameters of electrochemistry derived from the Tafel curves are shown in Table 1, where R_p is the polarization resistance of the material., The anodic slope, β_a , reflects the ease of the oxidation process, the cathodic slope, β_c , reflects the ease of the reduction reaction, E_{Corr} indicates the material's susceptibility to corrode, and I_{Corr} is directly related to the material's corrosion rate (Castro et al. 2025; John et al.2015). The final two parameters, corrosion inhibition efficiency (% IE) and corrosion rate CR, are determined using Equation (1) (Zhang et al. 2009).

$$E\% = \left(1 - \frac{i}{i_0}\right) \times 100 \dots\dots\dots(1)$$

Where the unconstrained and inhibited corrosion current densities are denoted by i_0 and i , respectively.

The samples' corrosion characteristics are displayed in Table 3. The two carbon steels' polarization resistance and potential were improved by the coated films., as indicated by the data in Table 3. The maximum polarization potential was discovered in the ZnO coated API 5CL grade B and API 5CT N80 steels.

By blocking oxygen, zinc coating offers cathodic protection. Preventing moisture from touch with the steel surface directly, is one of the best ways to stop corrosion on steel (Owoeye et al. 2023; Owoeye et al. 2021).

Because zinc has a reduced reduction potential than steel, Zinc is the main component of mild steel, as shown by the FTIR and EDX spectra. By adding zinc to the steel's surface, corrosion resistance may be increased.

Zinc is a more active metal on steel surfaces due to its greater reduction potential.; They rust before iron, even if their coating fails. The material's surface is protected by ZnO thin film coatings.might have improved the steel's corrosion resistance (Owoeye et al. 2025).

Table 3. Potentiodynamic polarization parameters for API 5CT N80 and API 5CL Grade B steels coated by thin film ZnO in albian water.

Steel		E _{corr} (mv)	R _P (Kohm. cm ²)	I _{corr} (μAcm. ⁻²)	ba (mv)	- bC (mv)	CR (μm/y)	E (%)
API 5CT N80	untreated	-671,6	1.08	10.7656	60.1	103.6	125.9	/
	Coated with ZnO	-563.7	9.57	1.2787	73.6	79.6	14.95	88.12
API 5L Grade B	untreated	-683.1	1.39	11.8511	60.2	143.6	138.6	/
	Coated with ZnO	-544.8	20.83	0.5456	52.9	95.4	6.381	95.39

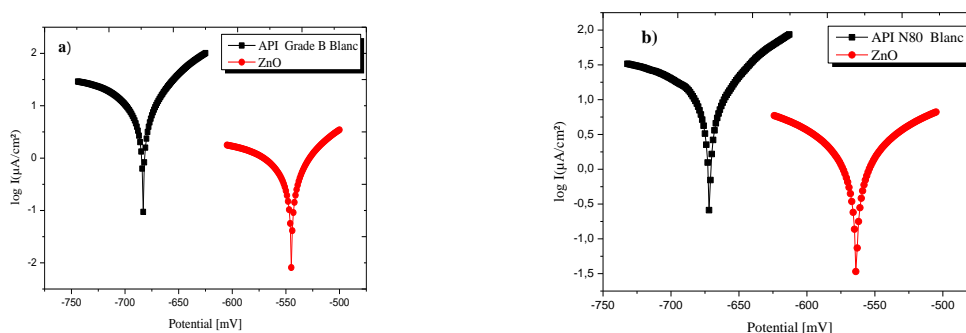


Fig.5. Polarization curves for without and with ZnO thin films in albian water at ambient temperatures: a) API 5CT N80 steel B) API 5L Grade B

4. Conclusions

Spray pyrolysis was used to apply ZnO thin layers to carbon steel. The films that are coated substitutional diffusion into The SEM data showed that the carbonsteel substrate had improved surface morphology.. EDX and FTIR results confirmed that deposited O and Zn were present in the deposited films. ZnO coating for two different steels resulted in increased strength and hardness. It was discovered that the deposited layers suppressed the signal of the Fe concentration of the carbon steel, which significantly impacted the corrosion resistance of the material. When ZnO thin films were applied to carbon steel, The steel's polarization curve marginally moved toward more potentials for polarization. This implies that The steel's resistance to corrosion was enhanced by the coated coatings., where corrosion inhibition efficiency (%IE) of API 5CL Grade B and API 5CT N 80 equals respectively 95.39 % and 88.12 %

To investigate the coatings' long-term stability, more research should be done on how coated ZnO affects corrosion resistance in various corrosive conditions, such as salty and acidic, and at different temperatures.

Acknowledgements

The authors sincerely acknowledged to the Scientific and Technical Research Center in Physico-Chemical Analysis (CRAPC), University of Kasdi Merbah, Ouargla , Algeria and Laboratory of Radiation and Plasmas and Physical Surface (LRPPS), the Kasdi Merbah University, Ouargla, 30000 Algeria , for their support of this study.

Competing Interests

Direction Générale de la Recherche Scientifique et du Développement Technologique

References

- [1] Heakal, F. E. T., et al. (2018). Performance of *Centaurea cyanus* aqueous extract towards corrosion mitigation of carbon steel in saline formation water. *Desalination*, 425, 111–122. <https://doi.org/10.1016/j.desal.2017.10.019>
- [2] Liu, H., et al. (2016). Corrosion inhibition of carbon steel in CO₂-containing oilfield produced water in the presence of iron-oxidizing bacteria and inhibitors. *Corrosion Science*, 109, 149–160. <https://doi.org/10.1016/j.corsci.2016.01.012>
- [3] Usher, K. M., et al. (2014). Critical review: Microbially influenced corrosion of buried carbon steel pipes. *International Biodeterioration & Biodegradation*, 93, 84–106. <https://doi.org/10.1016/j.ibiod.2014.05.007>
- [4] Chen, Z., et al. (2012). Benzotriazole as a volatile corrosion inhibitor during the early stage of copper corrosion under adsorbed thin electrolyte layers. *Corrosion Science*, 65, 214–222. <https://doi.org/10.1016/j.corsci.2012.08.019>
- [5] Benamor, A., et al. (2018). Effect of temperature and fluid speed on the corrosion behavior of carbon steel pipeline in Qatari oilfield produced water. *Journal of Electroanalytical Chemistry*, 808, 218–227. <https://doi.org/10.1016/j.jelechem.2017.12.009>
- [6] Cheng-hong, P., et al. (2012). Failure analysis of a steel tube joint perforated by corrosion in a well-drilling pipe. *Engineering Failure Analysis*, 25, 13–28. <https://doi.org/10.1016/j.engfailanal.2012.04.003>
- [7] Alamilla, J. L., et al. (2013). Failure analysis and mechanical performance of an oil pipeline. *Materials & Design*, 50, 766–773. <https://doi.org/10.1016/j.matdes.2013.03.055>
- [8] Tang, P., et al. (2009). Failure analysis and prediction of pipes due to the interaction between multiphase flow and structure. *Engineering Failure Analysis*, 16(5), 1749–1756. <https://doi.org/10.1016/j.engfailanal.2009.01.002>
- [9] Zhang, M. M., & Katz, J. (2010). Enhancement of channel wall vibration due to acoustic excitation of an internal bubbly flow. *Journal of Fluids and Structures*, 26(6), 994–1017. <https://doi.org/10.1016/j.jfluidstructs.2010.06.003>
- [10] Finšgar, M., & Jackson, J. (2014). Application of corrosion inhibitors for steels in acidic media for the oil and gas industry: A review. *Corrosion Science*, 86, 17–41. <https://doi.org/10.1016/j.corsci.2014.04.044>

- [11] Barmatov, E., et al. (2012). Research on corrosion inhibitors for acid stimulation. *Corrosion*, 2012-1573. <https://doi.org/10.5006/C2012-01573>
- [12] Jordan, M. M., et al. (2001). Deployment of a scale squeeze enhancer and oil-soluble scale inhibitor to avoid oil production losses in low water-cut well. *SPE Production & Facilities*, 16(04), 267–276. <https://doi.org/10.2118/74330-PA>
- [13] Migahed, M. A., et al. (2015). Corrosion inhibition of X-65 carbon steel in oil wells produced water under CO₂ environment. *International Journal of Electrochemical Science*, 10(2), 1343–1360. [https://doi.org/10.1016/S1452-3981\(23\)05076-9](https://doi.org/10.1016/S1452-3981(23)05076-9)
- [14] Yadav, M., et al. (2016). Nontoxic corrosion inhibitors for N80 steel in hydrochloric acid. *Arabian Journal of Chemistry*, 9(2), S1487–S1495. <https://doi.org/10.1016/j.arabjc.2012.03.011>
- [15] Vishwanatham, S., & Haldar, N. (2008). Furfuryl alcohol as corrosion inhibitor for N80 steel in hydrochloric acid. *Corrosion Science*, 50(11), 2999–3004. <https://doi.org/10.1016/j.corsci.2008.08.005>
- [16] Zhu, S. D., et al. (2011). Corrosion of N80 carbon steel in oil field formation water containing CO₂ in the absence and presence of acetic acid. *Corrosion Science*, 53(10), 3156–3165. <https://doi.org/10.1016/j.corsci.2011.05.059>
- [17] Heakal, F. E. T., & Elkholy, A. E. (2017). Gemini surfactants as corrosion inhibitors for carbon steel. *Journal of Molecular Liquids*, 230, 395–407. <https://doi.org/10.1016/j.molliq.2017.01.047>
- [18] Peabody, A. W. (2001). *Peabody's control of pipeline corrosion* (2nd ed.). NACE International.
- [19] Nagarajan, S., et al. (2012). Nanocomposite coatings on biomedical grade stainless steel for improved corrosion resistance and biocompatibility. *ACS Applied Materials & Interfaces*, 4, 5134–5141. <https://doi.org/10.1021/am301559r>
- [20] Verma, C., et al. (2017). Ionic liquids as green and sustainable corrosion inhibitors for metals and alloys: An overview. *Journal of Molecular Liquids*, 233, 403–414. <https://doi.org/10.1016/j.molliq.2017.02.111>
- [21] Barmatov, E., et al. (2012). Research on corrosion inhibitors for acid stimulation. *Corrosion*. <https://doi.org/10.5006/C2012-01573>
- [22] Jordan, M. M., et al. (2001). Deployment of a scale squeeze enhancer and oil-soluble scale inhibitor to avoid oil production losses in low water-cut well. *SPE Production & Facilities*, 16(4), 267–276. <https://doi.org/10.2118/74330-PA>
- [23] Migahed, M. A., et al. (2015). Corrosion inhibition of X-65 carbon steel in oil wells produced water under CO₂ environment. *International Journal of Electrochemical Science*, 10(2), 1343–1360. [https://doi.org/10.1016/S1452-3981\(23\)05076-9](https://doi.org/10.1016/S1452-3981(23)05076-9)
- [24] Yadav, M., et al. (2016). Nontoxic corrosion inhibitors for N80 steel in hydrochloric acid. *Arabian Journal of Chemistry*, 9(2), S1487–S1495. <https://doi.org/10.1016/j.arabjc.2012.03.011>
- [25] Vishwanatham, S., & Haldar, N. (2008). Furfuryl alcohol as corrosion inhibitor for N80 steel in hydrochloric acid. *Corrosion Science*, 50(11), 2999–3004. <https://doi.org/10.1016/j.corsci.2008.08.005>
- [26] Zhu, S. D., et al. (2011). Corrosion of N80 carbon steel in oil field formation water containing CO₂ in the absence and presence of acetic acid. *Corrosion Science*, 53(10), 3156–3165. <https://doi.org/10.1016/j.corsci.2011.05.059>
- [27] Heakal, F. E. T., & Elkholy, A. E. (2017). Gemini surfactants as corrosion inhibitors for carbon steel. *Journal of Molecular Liquids*, 230, 395–407. <https://doi.org/10.1016/j.molliq.2017.01.047>
- [28] Peabody, A. W. (2001). *Peabody's control of pipeline corrosion* (2nd ed.). NACE International.
- [29] Nagarajan, S., et al. (2012). Nanocomposite coatings on biomedical grade stainless steel for improved corrosion resistance and biocompatibility. *ACS Applied Materials & Interfaces*, 4, 5134–5141. <https://doi.org/10.1021/am301559r>
- [30] Verma, C., et al. (2017). Ionic liquids as green and sustainable corrosion inhibitors for metals and alloys: An overview. *Journal of Molecular Liquids*, 233, 403–414. <https://doi.org/10.1016/j.molliq.2017.02.111>
- [31] Benkrima, Y., et al. (2022). A first-principles investigation into the electronic characteristics of phase changes in ZnO at high pressures. *Journal of Ovonic Research*, 18, 797–804. <https://doi.org/10.15251/JOR.2022.186.797>
- [32] Owoeye, V. A., et al. (2025). Microstructure and corrosion resistance of pyrolyzed Mg–ZnO thin film coatings on mild steel. *Inorganic Materials*, 5, 100085. <https://doi.org/10.1016/j.cinorg.2024.100085>
- [33] Owoeye, V. A., et al. (2023). SCAPS 3201 simulation of tunable heterostructured p-CdTe and n-CdS thin films-based solar cells. *Results in Engineering*, 18, 101039. <https://doi.org/10.1016/j.rineng.2023.101039>
- [34] Owoeye, V. A., et al. (2021). Microstructure and anti-corrosion properties of spray pyrolyzed Ni-doped ZnO thin films for multifunctional surface protection applications. *Engineering Research Express*, 3, 025012. <https://doi.org/10.1088/2631-8695/abf65f>
- [35] Park, J. Y., et al. (2005). Size control of ZnO nanorod arrays grown by metalorganic chemical vapour deposition. *Nanotechnology*, 16, 2044. <https://doi.org/10.1088/0957-4484/16/10/010>
- [36] Owoeye, V. A., et al. (2019). Microstructural and optical properties of Ni-doped ZnO thin films prepared by chemical spray pyrolysis technique. *Materials Research Express*, 6, 086455. <https://doi.org/10.1088/2053-1591/ab26d9>
- [37] Thirugnanam, T. (2013). Effect of Polymers (PEG and PVP) on Sol-Gel Synthesis of Microsized Zinc Oxide. *Journal of Nanomaterials*, 2013, 43–49. <https://doi.org/10.1155/2013/362175>
- [38] Rao, N. S., & Rao, M. V. B. (2015). Structural and optical investigation of ZnO nanopowders synthesized from zinc chloride and zinc nitrate. *American Journal of Materials Science*, 5, 66–68. <https://doi.org/10.5923/j.materials.20150503.02>
- [39] Quadri, W. T., et al. (2017). Zinc oxide nanocomposites of selected polymers: Synthesis, characterization, and corrosion inhibition studies on mild steel in HCl solution. *ACS Omega*, 2, 8421–8437. <https://doi.org/10.1021/acsomega.7b01385>
- [40] Raja, K., et al. (2014). Synthesis, structural and optical properties of ZnO and Ni-doped ZnO hexagonal nanorods by Co-precipitation method. *Spectrochimica Acta Part A: Molecular and Biomolecular Spectroscopy*, 120, 19–24. <https://doi.org/10.1016/j.saa.2013.09.103>

- [41] Tu, S., et al. (2025). Gleditsia sinensis extract as green corrosion inhibitor for N80 steel in 1 M HCl. *Journal of Molecular Structure*, 1321, 139890. <https://doi.org/10.1016/j.molstruc.2024.139890>
- [42] Köck, E. M., et al. (2013). In situ FT-IR spectroscopic study of CO₂ and CO adsorption on Y₂O₃, ZrO₂ and yttria-stabilized ZrO₂. *Journal of Physical Chemistry C*, 117, 17666–17673. <https://doi.org/10.1021/jp405625x>
- [43] Zhang, Y., et al. (2018). Facile fabrication of zinc oxide coated superhydrophobic and superoleophilic meshes for efficient oil/water separation. *RSC Advances*, 8, 35150–35156. <https://doi.org/10.1039/C8RA06059B>
- [44] Pujari, S., et al. (2025). Polyoxometalate/ α -Fe₂O₃/polyaniline composite: Tailored approaches for high-performance supercapacitors. *Journal of Alloys and Compounds*, 1010, 177306. <https://doi.org/10.1016/j.jallcom.2024.177306>
- [45] Xu, R., et al. (2008). Effects of rare earth on microstructures and properties of Ni-WP-CeO₂-SiO₂ nano-composite coatings. *Journal of Rare Earths*, 26(4), 579–583. [https://doi.org/10.1016/S1002-0721\(08\)60141-6](https://doi.org/10.1016/S1002-0721(08)60141-6)
- [46] Chikodi, D. M. C., et al. (2021). Anti-wear and hardness values of functional value-added Zn-ZnO-rice husk ash composite coating of mild steel. *Advanced Composite Materials*, 30(1), 27–32. <https://doi.org/10.18280/rcma.310104>
- [47] Sobhanardakani, S., et al. (2018). Removal of heavy metal (Hg(II) and Cr(VI)) ions from aqueous solutions using Fe₂O₃@SiO₂ thin films as a novel adsorbent. *Process Safety and Environmental Protection*, 120, 348–357. <https://doi.org/10.1016/j.psep.2018.10.002>
- [48] Castro, M. A. M., et al. (2025). Increased corrosion resistance of steel substrates coated with epoxy resin/ZnO/Fe₂O₃ obtained from electric arc furnace dust recovery. *Journal of Materials Research and Technology*, 36, 9462–9472. <https://doi.org/10.1016/j.jmrt.2025.05.128>
- [49] Zhang, Q. B., et al. (2009). Corrosion inhibition of mild steel by alkyylimidazolium ionic liquids in hydrochloric acid. *Electrochimica Acta*, 54(6), 1881–1887. <https://doi.org/10.1016/j.electacta.2008.10.025>
- [50] John, S., et al. (2015). Enhancement of corrosion protection of mild steel by chitosan/ZnO nanoparticle composite membranes. *Progress in Organic Coatings*, 84, 28–34. <https://doi.org/10.1016/j.porgcoat.2015.02.005>